Chapter 2

SOLAR ULTRAVIOLET IRRADIANCE

Section 2.1 L.A. Hall
Sections 2.2–2.8 L.J. Heroux and H.E. Hinteregger

2.1 SOLAR UV IRRADIANCE IN THE STRATOSPHERE

2.1.1 Solar Spectrum Between 2000 and 3000 Å

Solar radiation incident on the earth's atmosphere is absorbed in the spectral range 2000-3000 Å by stratospheric ozone in the Hartley band. This absorption is an almost structureless continuum having a maximum near 2550 Å and falling almost symmetrically on both sides. The absorption of solar radiation in this range provides the energy for stratospheric photochemistry and is the major part of the heat input which produces the local temperature maximum in the stratopause around 50 km.

Measurements of the 2000-3000 Å spectrum in the stratosphere can be made up to about 40 km by means of high-altitude balloons. Only about 3% of the total ozone column density remains above 40 km; but at 2550 Å where the absorption coefficient of ozone peaks, only 3% of the incident solar radiation penetrates to 40 km at local noon and 30° latitude. This can be seen in Figure 2-1, where the bowl-shaped depression between 2900 and 2200 Å is caused by ozone absorption (see Chapter 21).

Table 2-1 gives the solar spectrum in 1-angstrom averages from a measurement made on 19 April 1978 at Holloman AFB, N.M. The data in Table 2-1 were taken at a balloon float altitude of 41.4 km at 1022 h local time. The solar zenith angle was 29.6° and the ozone column density above 41.4 km was about 2.7 × 10^{17} molecules/cm^2. Further details and a description of the instrumentation and its calibration are given by Hall [1981].

2.2 SOLAR CONSTANT AND SPECTRAL IRRADIANCE

2.2.1 Solar Constant

The solar constant S is the total solar radiative energy at the top of the earth's atmosphere corrected for the mean sun-earth distance. The solar constant or total solar irradiance expressed in units of watts per square meter (W/m^2) is the largest contributor to the earth's energy budget. There have been several measurements of the solar constant as summarized by Frohlich [1977]. The most probable value for S proposed by Frohlich is S = 1373 ± 20 W/m^2.

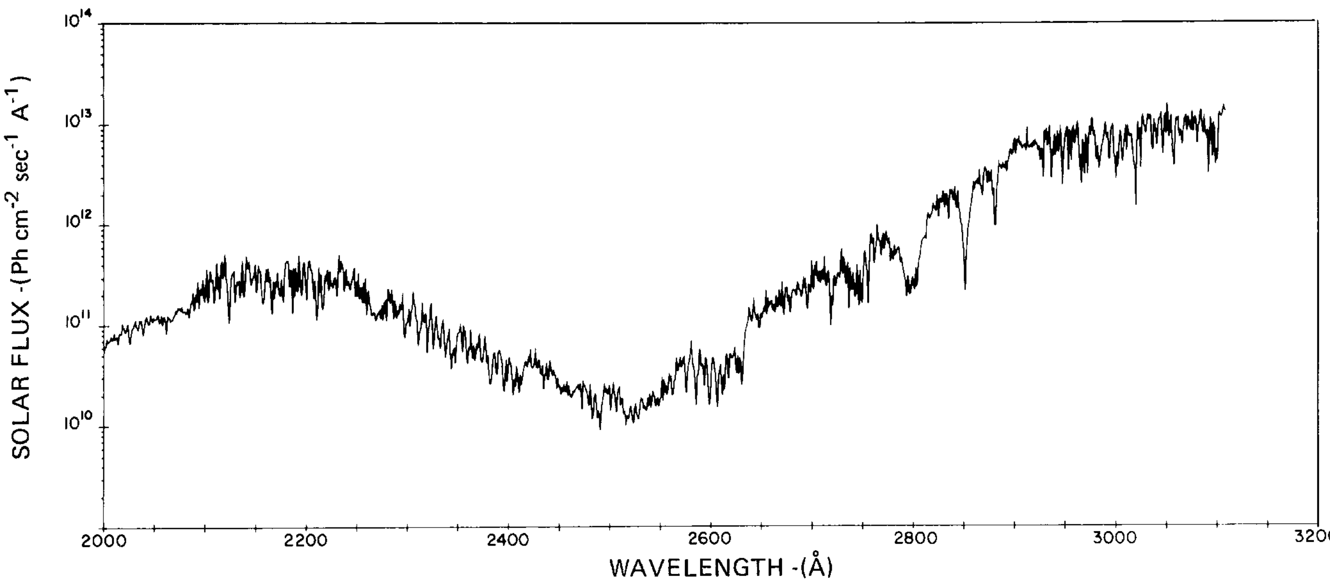

Figure 2-1. The solar irradiance in 1-Å intervals at 39.5 km in the stratosphere. Measurements made on 21 April 1977 with a solar zenith angle of 31° [Hall, 1981].

Table 2-1. Solar irradiance at 40 km.

	One Angstrom averages centered on the wavelength in units of 10^{11} ph cm^{-2} s^{-1} Å^{-1}									
Å	0	1	2	3	4	5	6	7	8	9
2000	0.470	0.551	0.519	0.688	0.649	0.623	0.661	0.748	0.674	0.695
10	0.802	0.623	0.727	0.678	0.642	0.821	0.760	0.766	1.03	0.934
20	0.907	0.809	0.897	0.983	1.00	0.648	0.613	0.827	0.861	0.940
30	1.04	1.09	0.909	0.952	0.929	1.13	0.950	1.13	0.905	0.732
40	0.879	1.15	1.21	1.05	1.01	0.968	1.25	1.08	1.13	1.09
50	1.09	1.23	1.09	1.30	1.10	0.943	1.21	1.26	0.981	1.15
60	1.16	1.07	0.754	1.20	1.14	1.12	1.04	1.02	1.12	1.25
70	1.27	1.36	1.35	1.42	1.36	1.54	1.39	1.55	1.29	1.35
80	1.34	1.30	1.32	1.43	1.21	1.35	1.70	1.51	2.22	1.39
90	1.50	1.99	1.86	2.61	1.71	2.06	2.22	2.00	2.72	2.05
2100	1.58	2.62	3.75	1.68	1.86	3.56	3.07	3.21	2.41	1.78
10	1.74	3.28	4.27	2.04	3.01	1.95	4.17	4.49	3.22	3.14
20	5.31	3.42	2.79	2.00	1.04	1.78	3.29	3.06	3.18	3.43
30	1.79	2.81	2.39	3.02	2.67	1.84	2.83	4.11	2.89	1.71
40	2.61	5.13	3.78	4.11	4.15	3.33	2.85	2.91	2.98	4.04
50	3.40	2.55	2.81	4.16	3.50	3.51	2.93	1.84	1.80	1.85
60	2.74	3.78	2.94	3.72	2.78	2.99	1.51	1.40	3.07	1.63
70	2.94	2.67	3.51	2.73	2.27	1.76	2.89	2.47	1.54	3.60
80	4.27	4.53	4.40	4.45	2.60	3.76	3.33	1.58	3.92	1.98
90	4.16	2.90	2.27	5.54	4.38	2.85	1.92	3.18	4.66	4.34
2200	3.03	1.83	3.80	4.60	4.64	4.01	3.47	3.15	1.68	3.18
10	1.55	1.10	1.74	4.23	2.26	3.34	2.17	1.26	1.60	3.20
20	3.29	3.67	3.85	2.32	3.64	3.13	2.60	2.49	3.40	3.10
30	3.04	2.01	4.06	5.33	4.42	4.65	4.52	4.12	2.75	3.27
40	4.20	2.86	3.25	2.73	2.20	3.48	3.29	4.04	4.00	2.43
50	2.97	2.22	3.37	2.65	2.13	2.82	2.12	2.90	2.12	3.41
60	1.44	2.12	2.62	1.76	1.78	1.45	1.60	1.33	1.57	1.25
70	1.34	1.47	1.40	1.79	1.35	1.92	1.28	1.86	1.90	2.17
80	1.39	2.75	2.87	1.95	2.12	2.83	2.02	1.18	2.30	1.94
90	1.45	1.61	1.75	1.79	1.89	1.77	2.58	1.08	0.858	1.25
2300	1.30	1.42	1.85	1.08	1.80	1.98	2.62	2.39	1.87	1.54
10	1.33	0.838	1.03	1.01	0.957	2.18	1.50	1.44	1.68	1.56
20	0.624	1.09	1.40	2.10	2.01	1.18	0.768	0.954	1.42	1.56
30	1.25	1.11	0.914	0.659	1.24	1.13	1.67	0.954	0.577	0.714
40	0.914	1.09	1.19	0.565	0.451	0.626	0.718	0.784	0.489	0.758
50	1.17	0.974	1.24	1.49	1.10	0.653	1.38	1.17	1.17	0.628
60	0.505	0.815	0.785	1.22	0.744	0.601	0.838	0.522	0.719	0.717
70	0.887	0.937	1.11	0.704	0.457	0.626	0.721	0.993	0.846	0.525
80	0.604	0.374	0.281	0.279	0.448	0.631	0.665	0.683	0.430	0.323
90	0.583	0.831	0.583	0.637	0.549	0.279	0.200	0.365	0.542	0.276
2400	0.472	0.567	0.479	0.496	0.322	0.193	0.340	0.210	0.430	0.442
10	0.363	0.190	0.346	0.327	0.317	0.428	0.484	0.540	0.516	0.471
20	0.589	0.592	0.702	0.456	0.449	0.479	0.507	0.736	0.529	0.444
30	0.535	0.585	0.436	0.392	0.496	0.242	0.397	0.410	0.518	0.340
40	0.359	0.542	0.507	0.434	0.390	0.448	0.391	0.361	0.271	0.332
50	0.319	0.285	0.234	0.286	0.243	0.299	0.256	0.256	0.335	0.234
60	0.299	0.252	0.206	0.220	0.257	0.234	0.267	0.272	0.291	0.321
70	0.270	0.304	0.294	0.140	0.366	0.307	0.316	0.280	0.259	0.209
80	0.197	0.315	0.239	0.109	0.134	0.211	0.267	0.215	0.123	0.161
90	0.121	0.073	0.165	0.204	0.249	0.340	0.268	0.300	0.271	0.278

Table 2-1. (*Continued*)

	One Angstrom averages centered on the wavelength in units of 10^{11} ph cm^{-2} s^{-1} Å^{-1}									
Å	0	1	2	3	4	5	6	7	8	9
2500	0.323	0.151	0.241	0.289	0.326	0.292	0.218	0.129	0.245	0.294
10	0.346	0.185	0.235	0.234	0.146	0.159	0.104	0.144	0.138	0.109
20	0.188	0.183	0.168	0.117	0.117	0.172	0.186	0.173	0.129	0.101
30	0.162	0.244	0.229	0.224	0.185	0.200	0.159	0.171	0.229	0.193
40	0.269	0.169	0.224	0.282	0.276	0.259	0.184	0.227	0.254	0.197
50	0.200	0.249	0.410	0.221	0.410	0.270	0.342	0.255	0.349	0.495
60	0.371	0.417	0.297	0.262	0.339	0.394	0.689	0.418	0.564	0.575
70	0.725	0.509	0.593	0.681	0.682	0.413	0.288	0.509	0.594	0.623
80	0.856	0.962	0.781	0.441	0.641	0.370	0.189	0.422	0.470	0.788
90	0.866	0.561	0.558	0.529	0.320	0.685	0.605	0.526	0.258	0.195
2600	0.243	0.510	0.685	0.663	0.515	0.504	0.291	0.191	0.425	0.493
10	0.566	0.393	0.251	0.435	0.300	0.696	0.722	0.554	0.415	0.692
20	0.772	0.696	0.528	0.841	0.796	0.665	0.436	0.666	0.462	0.640
30	0.597	0.346	0.473	0.781	1.23	1.23	1.45	1.60	2.14	2.08
40	1.60	1.66	1.71	2.75	1.99	1.85	1.63	1.84	1.33	1.31
50	1.84	1.63	1.84	2.15	2.05	3.06	1.86	2.49	2.29	2.14
60	2.53	2.43	1.82	2.39	1.63	2.63	2.25	1.90	3.07	2.50
70	1.96	3.74	1.90	1.78	3.40	3.17	3.21	2.18	2.71	1.65
80	2.48	3.16	2.88	2.90	2.96	2.57	3.61	3.30	2.94	3.00
90	2.36	2.90	3.94	3.10	3.76	2.16	1.94	3.44	2.90	2.70
2700	5.25	4.00	2.96	5.02	3.74	5.70	3.86	3.62	4.34	3.19
10	4.45	4.35	3.79	5.92	2.91	3.27	3.98	4.62	3.49	1.21
20	2.44	1.81	3.78	4.08	2.89	3.58	4.13	3.96	3.48	6.37
30	6.98	4.15	5.56	4.42	3.52	4.30	5.25	1.63	4.18	3.32
40	2.47	3.90	3.14	2.20	2.55	4.65	3.55	1.73	4.11	2.38
50	2.03	4.25	6.45	6.19	4.60	4.22	1.80	4.23	8.10	9.87
60	7.34	8.71	4.90	6.28	7.22	11.7	9.70	7.86	7.55	6.31
70	9.44	10.4	7.00	10.3	10.6	9.03	8.83	8.22	5.85	7.13
80	5.79	5.78	7.57	6.18	6.61	7.15	7.38	6.95	5.01	5.86
90	4.79	4.10	3.81	3.31	2.44	3.68	4.43	2.38	2.59	3.59
2800	3.79	3.07	2.56	5.27	2.95	3.97	5.39	5.61	7.01	8.34
10	8.58	8.87	8.80	8.66	12.9	15.7	14.2	13.8	15.0	15.7
20	19.1	17.1	18.0	15.7	22.7	21.1	13.9	21.1	19.5	19.7
30	24.4	24.6	17.8	26.6	23.3	19.1	12.4	24.9	23.9	26.0
40	21.9	19.0	26.7	18.4	15.8	25.4	17.2	14.7	11.9	10.9
50	7.65	5.92	2.60	4.87	7.64	10.8	12.2	15.8	18.7	21.5
60	29.5	24.4	31.8	28.1	30.7	29.3	38.0	27.1	26.5	21.8
70	33.6	40.8	42.1	39.7	24.6	37.9	30.3	33.7	38.4	22.3
80	25.1	12.2	10.2	24.2	29.0	47.5	41.4	41.8	39.2	44.9
90	40.2	38.0	50.4	34.8	47.7	46.7	62.4	60.3	54.6	59.9
2900	73.1	80.5	54.4	69.0	75.2	83.2	67.7	70.0	61.5	64.8
10	65.1	64.6	58.9	101	67.3	63.0	62.3	71.6	55.8	71.9
20	67.4	73.5	72.2	70.9	55.2	65.8	48.9	60.1	59.2	32.3
30	91.7	76.2	92.1	69.4	71.6	98.9	74.4	26.9	62.6	51.6
40	83.4	55.7	62.5	91.3	63.8	66.6	103	70.7	26.1	42.3
50	63.2	87.9	92.0	105	31.6	90.5	87.0	57.2	85.7	102
60	73.1	73.7	97.7	112	87.0	42.9	53.2	26.0	77.7	70.1
70	34.5	69.9	79.8	39.0	71.9	106	81.6	113	123	85.4
80	86.0	67.8	41.8	68.1	34.6	45.3	51.7	63.2	67.3	76.0
90	110	106	87.0	82.9	56.9	40.3	94.0	92.4	110	69.1

Table 2-1. *(Continued)*

Å	0	1	2	3	4	5	6	7	8	9
	One Angstrom averages centered on the wavelength in units of 10^{11} ph cm^{-2} s^{-1} Å^{-1}									
3000	46.3	25.8	61.7	36.8	57.2	93.5	90.1	54.5	46.8	65.9
10	69.0	110	54.5	101	85.2	82.8	83.4	89.5	54.6	45.2
20	48.5	14.7	62.1	109	76.4	97.4	41.2	108	133	104
30	100	93.5	104	139	120	118	132	78.3	43.3	112
40	117	86.5	66.3	96.3	120	121	138	79.3	50.0	108
50	134	80.8	168	142	79.0	96.0	126	83.0	44.9	44.2
60	90.7	111	117	129	77.0	89.2	101	63.8	83.7	114
70	123	121	96.2	109	122	109	78.6	134	107	107
80	125	115	67.6	103	101	144	150	96.9	77.3	134
90	85.1	81.2	90.6	30.5	73.2	117	113	47.4	96.9	105

Two rocket flight measurements of the solar irradiance were also reported by Willson et al. [1980]. The total solar flux measurement for 29 June 1976 was 1368.1 ± 0.5 W/m^2 and for 16 November 1978 was 1373.4 ± 0.5 W/m^2. These measurements are within the error estimates of Frohlich.

The solar spectral irradiance S $\Delta\lambda$, defined as the irradiance per wavelength interval $\Delta\lambda$, is plotted in Figure 2-2 for wavelengths longer than 3000 Å. This figure is based on data from Labs and Neckel between 3000 Å and 3 μm, and Thekaekara above 3 μm. These sources of data are from

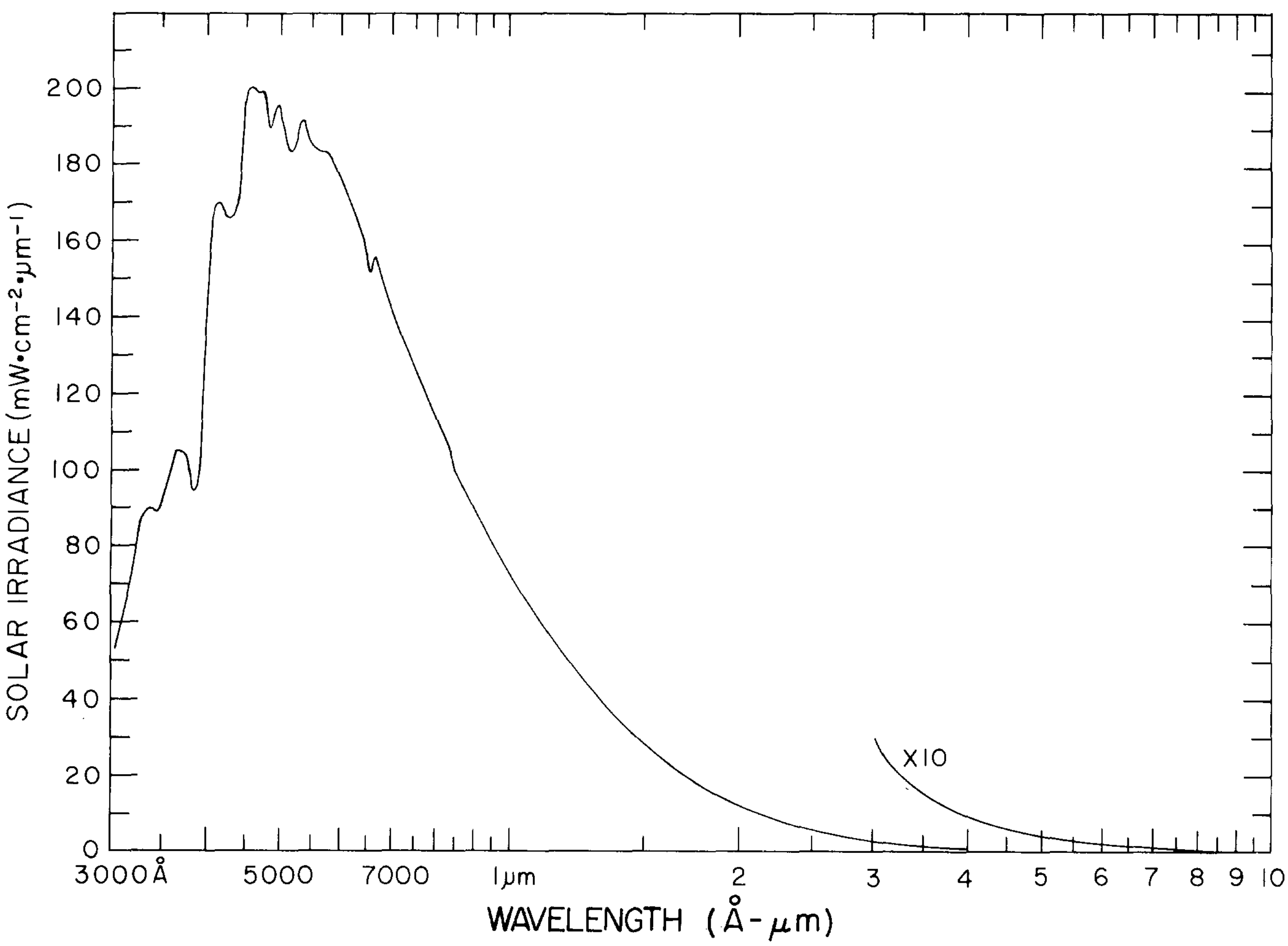

Figure 2-2. The solar spectral irradiance for wavelengths longer than 3000 Å. Th᷉ data between 3000 Å and 3 μm are from Labs and Neckel and from Thekaekara above 3 μm. These data are from a summary given by Pierce and Allen [1977].

a summary given by Pierce and Allen [1977]. The spectral region above 3000 Å accounts for approximately 99% of the solar constant. Nearly all of this energy reaches the surface of the earth since atmospheric absorption of the radiation is negligible. The irradiance in this wavelength region does not appear to vary with solar activity. Because this region is the principal source of solar energy, the variation in the total solar irradiance or solar constant is also small and is now believed to be less than ± 1%.

2.2.2 Solar Irradiance Between 1 and 3000 Å For Solar Minimum

The solar spectral irradiance for wavelengths below 3180 Å at the top of the earth's atmosphere is tabulated in Table 2-2 for 10 Å wavelength intervals. The values of irradiance for the wavelength range 1 to 2300 Å are for levels of solar activity near the minimum value of activity for the 11-year solar cycle. The irradiance values between 1 and 10 Å are from Kreplin [1977], between 10 and 50 Å from Manson [1977], and between 50 and 1850 Å from the solar minimum reference spectrum of Heroux and Hinteregger [1978]. The irradiance between 1850 and 2090 Å from Semain and Simon and between 2090 and 2300 Å from Simon is from a summary of Delaboudiniere et al. [1978]. The irradiance between 2300 and 3150 Å was measured by Mount and Rottman [1981] in a rocket flight flown near solar maximum of the present solar cycle 21. However, because the spectral irradiance in this longer UV wavelength region does not vary significantly with solar activity, these irradiance values should also represent solar minimum conditions. In Table 2-2, the solar spectral irradiance is given in units of photons $cm^{-2}s^{-1}$ and in units of mW/m^2, which is also equivalent to ergs $cm^{-2}s^{-1}$. The fourth column in Table 2-2 gives the percentage of the total solar irradiance, $s = 1373\ W/m^2$,

Table 2-2. Solar irradiance and cumulative irradiance for quiet sun at the top of the earth's atmosphere. $S = 1373\ W/m^2$, $1\ mWm^{-2} = 1\ erg\ cm^{-2}\ s^{-1}$

Wavelength Interval Å	$\Phi_{\Delta\lambda}$ (10^9 photons $cm^{-2}\ s^{-1}$)	$S_{\Delta\lambda}$ mWm^{-2}	$\sum_0^\lambda S_{\Delta\lambda}/S$ %
1–10	0.0005	0.002	0.15×10^{-6}
10–20	0.0014	0.002	0.29
20–30	0.0076	0.006	0.73
30–40	0.088	0.050	4.4
40–50	0.095	0.042	7.4
1–50	0.193	0.102	
50–60	0.055	0.020	8.9×10^{-6}
60–70	0.069	0.021	1.0×10^{-5}
70–80	0.073	0.019	1.2
80–90	0.106	0.025	1.4
90–100	0.094	0.020	1.5
50–100	0.397	0.105	
100–110	0.048	0.009	1.6×10^{-5}
110–120	0.017	0.003	1.6
120–130	0.014	0.002	1.6
130–140	0.009	0.001	1.6
140–150	0.062	0.008	1.7
100–150	0.150	0.023	
150–160	0.082	0.011	1.8×10^{-5}
160–170	0.115	0.14	1.9
170–180	0.782	0.089	2.5
180–190	0.787	0.085	3.1
190–200	0.602	0.062	3.6
150–200	2.37	0.261	
200–210	0.292	0.029	3.8×10^{-5}
210–220	0.266	0.024	4.0

Table 2-2. (*Continued*)

Wavelength Interval Å	$\Phi_{\Delta\lambda}$ (10^9 photons cm^{-2} s^{-1})	$S_{\Delta\lambda}$ mWm^{-2}	$\sum_0^\lambda S_{\Delta\lambda}/S$ %
220–230	0.268	0.024	4.1
230–240	0.206	0.017	4.3
240–250	0.531	0.043	4.6
200–250	1.56	0.137	
250–260	1.233	0.095	5.3×10^{-5}
260–270	0.204	0.015	5.4
270–280	0.426	0.031	5.6
280–290	0.262	0.018	5.7
290–300	0.225	0.015	5.8
250–300	2.35	0.174	
300–310	7.700	0.504	9.5×10^{-5}
310–320	0.375	0.023	9.7
320–330	0.020	0.001	9.7
330–340	0.140	0.008	9.8
340–350	0.430	0.025	9.9
300–350	8.67	0.561	
350–360	0.110	0.006	1.0×10^{-4}
360–370	0.840	0.045	1.0
370–380	0.000	0.000	1.0
380–390	0.000	0.000	1.0
390–400	0.014	0.001	1.0
350–400	0.964	0.052	
400–410	0.161	0.008	1.0×10^{-4}
410–420	0.027	0.001	1.0
420–430	0.002	0.000	1.0
430–440	0.187	0.009	1.0
440–450	0.005	0.000	1.0
400–450	0.382	0.018	
450–460	0.009	0.000	1.0×10^{-4}
460–470	0.305	0.013	1.1
470–480	0.026	0.001	1.1
480–490	0.053	0.002	1.1
490–500	0.173	0.007	1.1
450–500	0.566	0.023	
500–510	0.163	0.006	1.1×10^{-4}
510–520	0.025	0.001	1.1
520–530	0.111	0.004	1.1
530–540	0.120	0.004	1.1
540–550	0.021	0.001	1.1
500–550	0.440	0.016	
550–560	0.786	0.028	1.1×10^{-4}
560–570	0.093	0.003	1.1
570–580	0.031	0.001	1.1

Table 2-2. (*Continued*)

Wavelength Interval Å	$\Phi_{\Delta\lambda}$ (10^9 photons cm^{-2} s^{-1})	$S_{\Delta\lambda}$ mWm^{-2}	$\sum_0^\lambda S_{\Delta\lambda}/S$ %
580–590	1.270	0.043	1.1
590–600	0.155	0.005	1.1
550–600	2.34	0.080	
600–610	0.530	0.017	1.1×10^{-4}
610–620	0.017	0.001	1.1
620–630	1.832	0.058	1.2
630–640	0.021	0.001	1.2
640–650	0.062	0.002	1.2
600–650	2.46	0.079	
650–660	0.026	0.001	1.2×10^{-4}
660–670	0.014	0.000	1.2
670–680	0.014	0.000	1.2
680–690	0.131	0.004	1.2
690–700	0.044	0.001	1.2
650–700	0.229	0.006	
700–710	0.369	0.010	1.2×10^{-4}
710–720	0.072	0.002	1.2
720–730	0.015	0.000	1.2
730–740	0.019	0.001	1.2
740–750	0.024	0.001	1.2
700–750	0.499	0.014	
750–760	0.117	0.003	1.2×10^{-4}
760–770	0.340	0.009	1.2
770–780	0.323	0.008	1.2
780–790	0.587	0.015	1.2
790–800	0.516	0.013	1.2
750–800	1.88	0.048	
800–810	0.111	0.003	1.2×10^{-4}
810–820	0.143	0.003	1.2
820–830	0.184	0.004	1.2
830–840	0.857	0.020	1.3
840–850	0.305	0.007	
800–850	1.60	0.037	
850–860	0.392	0.009	1.3×10^{-4}
860–870	0.504	0.012	1.3
870–880	0.643	0.015	1.3
880–890	0.833	0.019	1.3
890–900	1.071	0.024	1.3
850–900	3.44	0.079	
900–910	1.487	0.033	1.3×10^{-4}
910–920	0.502	0.011	1.4
920–930	0.274	0.006	1.4
930–940	0.447	0.009	1.4
940–950	0.408	0.009	1.4

Table 2-2. (*Continued*)

Wavelength Interval Å	$\Phi_{\Delta\lambda}$ (10^9 photons cm^{-2} s^{-1})	$S_{\Delta\lambda}$ mWm^{-2}	$\sum_0^\lambda S_{\Delta\lambda}/S$ %
900–950	3.12	0.068	
950–960	0.048	0.001	1.4×10^{-4}
960–970	0.058	0.001	1.4
970–980	5.069	0.103	1.5
980–990	0.253	0.005	1.5
990–1000	0.439	0.009	1.5
950–1000	5.87	0.119	
1000–1010	0.119	0.002	1.5×10^{-4}
1010–1020	0.222	0.004	1.5
1020–1030	3.671	0.071	1.5
1030–1040	3.794	0.073	1.6
1040–1050	0.244	0.005	1.6
1000–1050	8.05	0.155	
1050–1060	0.292	0.006	1.6×10^{-4}
1060–1070	0.405	0.008	1.6
1070–1080	0.528	0.010	1.6
1080–1090	1.021	0.019	1.6
1090–1100	0.599	0.011	1.6
1050–1100	2.85	0.054	
1100–1110	0.083	0.001	1.6×10^{-4}
1110–1120	0.022	0.000	1.6
1120–1130	0.679	0.012	1.6
1130–1140	0.045	0.001	1.6
1140–1150	0.077	0.001	1.6
1100–1150	0.906	0.015	
1150–1160	0.129	0.002	1.6×10^{-4}
1160–1170	0.219	0.004	1.6
1170–1180	2.872	0.049	1.7
1180–1190	0.493	0.008	1.7
1190–1200	0.675	0.011	1.7
1150–1200	4.39	0.074	
1200–1210	4.855	0.080	1.7×10^{-4}
1210–1220	251.774	4.114	4.7
1220–1230	0.636	0.010	4.7
1230–1240	1.480	0.024	4.8
1240–1250	0.640	0.010	4.8
1200–1250	259.39	4.24	
1250–1260	1.080	0.017	4.8×10^{-4}
1260–1270	0.930	0.015	4.8
1270–1280	0.750	0.012	4.8
1280–1290	0.500	0.008	4.8
1290–1300	0.860	0.013	4.8

Table 2-2. (*Continued*)

Wavelength Interval Å	$\Phi_{\Delta\lambda}$ (10^9 photons cm^{-2} s^{-1})	$S_{\Delta\lambda}$ mWm^{-2}	$\sum_0^\lambda S_{\Delta\lambda}/S$ %
1250–1300	4.12	0.065	
1300–1310	4.585	0.070	4.9×10^{-4}
1310–1320	0.780	0.012	4.9
1320–1330	0.780	0.012	4.9
1330–1340	5.300	0.079	4.9
1340–1350	0.920	0.014	4.9
1300–1350	12.37	0.187	
1350–1360	1.47	0.022	5.0×10^{-4}
1360–1370	1.05	0.015	5.0
1370–1380	1.13	0.016	5.0
1380–1390	1.04	0.015	5.0
1390–1400	2.70	0.038	5.0
1350–1400	7.39	0.106	
1400–1410	2.70	0.038	5.1×10^{-4}
1410–1420	1.59	0.022	5.1
1420–1430	1.90	0.026	5.1
1430–1440	2.10	0.029	5.1
1440–1450	2.10	0.029	5.1
1400–1450	10.39	0.144	
1450–1460	2.30	0.031	5.2×10^{-4}
1460–1470	3.00	0.041	5.2
1470–1480	3.80	0.051	5.2
1480–1490	3.70	0.049	5.3
1490–1500	3.40	0.045	5.3
1450–1500	16.20	0.217	
1500–1510	3.90	0.051	5.3×10^{-4}
1510–1520	4.50	0.059	5.4
1520–1530	5.50	0.072	5.4
1530–1540	5.90	0.076	5.5
1540–1550	9.50	0.122	5.6
1500–1550	29.30	0.380	
1550–1560	8.80	0.113	5.6×10^{-4}
1560–1570	9.00	0.114	5.7
1570–1580	7.70	0.097	5.8
1580–1590	7.10	0.089	5.9
1590–1600	7.20	0.090	5.9
1550–1600	39.80	0.503	
1600–1610	7.90	0.098	6.0×10^{-4}
1610–1620	9.40	0.116	6.1
1620–1630	11.10	0.136	6.2
1630–1640	12.00	0.146	6.3
1640–1650	15.30	0.185	6.4

Table 2-2. *(Continued)*

Wavelength Interval Å	$\Phi_{\Delta\lambda}$ (10^9 photons cm^{-2} s^{-1})	$S_{\Delta\lambda}$ mWm^{-2}	$\sum_0^\lambda S_{\Delta\lambda}/S$ %
1600–1650	55.70	0.681	
1650–1660	25.00	0.300	6.6×10^{-4}
1660–1670	18.40	0.220	6.8
1670–1680	23.00	0.273	7.0
1680–1690	26.99	0.318	7.2
1690–1700	37.02	0.434	7.6
1650–1700	130.41	1.55	
1700–1710	43.00	0.501	7.9×10^{-4}
1710–1720	43.99	0.510	8.3
1720–1730	45.98	0.530	8.7
1730–1740	41.99	0.481	9.0
1740–1750	50.02	0.569	9.4
1700–1750	224.98	2.59	
1750–1760	56.99	0.645	9.9×10^{-4}
1760–1770	61.97	0.698	1.0×10^{-3}
1770–1780	74.02	0.828	1.1
1780–1790	80.99	0.901	1.2
1790–1800	82.96	0.908	1.2
1750–1800	356.93	3.99	
1800–1810	103.00	1.13	1.3×10^{-3}
1810–1820	126.00	1.38	1.4
1820–1830	132.02	1.44	1.5
1830–1840	131.96	1.43	1.7
1840–1850	110.95	1.20	1.7
1800–1850	603.93	6.57	
1850–1860	190.51	2.04	1.9×10^{-3}
1860–1870	237.55	2.53	2.1
1870–1880	265.25	2.81	2.3
1880–1890	279.95	2.95	2.5
1890–1900	293.84	3.08	2.7
1850–1900	1267.10	13.41	
1900–1910	293.48	3.06	2.9×10^{-3}
1910–1920	332.62	3.45	3.2
1920–1930	347.92	3.59	3.4
1930–1940	254.26	2.61	3.6
1940–1950	446.52	4.56	4.0
1900–1950	1674.80	17.27	
1950–1960	427.16	4.34	4.3×10^{-3}
1960–1970	485.73	4.91	4.6
1970–1980	487.21	4.90	5.0
1980–1990	492.68	4.93	5.3
1990–2000	552.41	5.50	5.7
1950–2000	2445.19	24.58	

Table 2-2. (*Continued*)

Wavelength Interval Å	$\Phi_{\Delta\lambda}$ (10^9 photons cm^{-2} s^{-1})	$S_{\Delta\lambda}$ mWm^{-2}	$\sum_0^\lambda S_{\Delta\lambda}/S$ %
2000–2010	624.83	6.19	6.2×10^{-3}
2010–2020	629.98	6.21	6.8
2020–2030	642.27	6.30	7.1
2030–2040	763.27	7.45	7.6
2040–2050	895.71	8.70	8.3
2000–2050	3556.06	34.85	
2050–2060	919.75	8.89	8.9×10^{-3}
2060–2070	964.77	9.28	9.6
2070–2080	1128.23	10.80	1.0×10^{-2}
2080–2090	1270.13	12.10	1.1
2090–2100	2562.98	24.30	1.3
2050–2100	6845.86	65.37	
2100–2110	$2.72 \times 10^{+3}$	25.6	1.5×10^{-2}
2110–2120	3.52	33.1	1.7
2120–2130	2.92	27.3	1.9
2130–2140	3.81	35.4	2.2
2140–2150	4.81	44.5	2.5
2100–2150	$17.78 \times 10^{+3}$	165.90	
2150–2160	$3.74 \times 10^{+3}$	34.5	2.8×10^{-2}
2160–2170	3.48	31.9	3.0
2170–2180	3.72	34.0	3.2
2180–2190	5.07	46.1	3.6
2190–2200	5.60	50.7	3.9
2150–2200	21.61×10^3	197.2	
2200–2210	5.42×10^3	48.8	4.3×10^{-2}
2210–2220	4.19	37.6	4.6
2220–2230	5.80	51.8	5.0
2230–2240	7.96	70.7	5.5
2240–2250	7.17	63.4	5.9
2200–2250	30.54×10^3	272.3	
2250–2260	6.95×10^3	61.2	6.4×10^{-2}
2260–2270	5.34	46.8	6.7
2270–2280	5.50	48.0	7.1
2280–2290	8.88	77.2	7.6
2290–2300	7.18	62.1	8.1
2250–2300	33.85×10^3	295.3	
2300–2310	6.88×10^3	59.3	8.5×10^{-2}
2310–2320	5.94	51.0	8.9
2320–2330	6.54	55.9	9.3
2330–2340	5.42	46.1	9.6
2340–2350	4.87	41.3	9.9
2300–2350	29.65×10^3	253.6	

Table 2-2. (*Continued*)

Wavelength Interval Å	$\Phi_{\Delta\lambda}$ (10^9 photons cm^{-2} s^{-1})	$S_{\Delta\lambda}$ mWm^{-2}	$\sum_0^\lambda S_{\Delta\lambda}/S$ %
2350–2360	6.78×10^3	57.2	1.0×10^{-1}
2360–2370	6.18	51.9	1.1
2370–2380	6.15	51.4	1.1
2380–2390	5.36	44.6	1.1
2390–2400	5.85	48.5	1.2
2350–2400	30.32×10^3	253.6	
2400–2410	5.10×10^3	42.1	1.2×10^{-1}
2410–2420	7.00	57.6	1.3
2420–2430	9.39	76.9	1.3
2430–2440	8.49	69.3	1.4
2440–2450	7.73	62.8	1.4
2400–2450	37.71×10^3	308.7	
2450–2460	6.46×10^3	52.3	1.4×10^{-1}
2460–2470	6.79	54.7	1.5
2470–2480	7.50	60.2	1.5
2480–2490	5.43	43.4	1.6
2490–2500	8.18	65.1	1.6
2450–2500	34.36×10^3	275.7	
2500–2510	7.66×10^3	60.7	1.6×10^{-1}
2510–2520	5.69	44.9	1.7
2520–2530	5.55	43.7	1.7
2530–2540	7.16	56.1	1.8
2540–2550	8.17	63.8	1.8
2500–2550	34.23×10^3	269.2	
2550–2560	11.2×10^3	87.1	1.9×10^{-1}
2560–2570	14.6	113	1.9
2570–2580	16.9	130	2.0
2580–2590	16.1	124	2.1
2590–2600	12.0	91.9	2.2
2550–2600	70.8×10^3	546	
2600–2610	11.9×10^3	90.7	2.3×10^{-1}
2610–2620	12.9	98.0	2.3
2620–2630	13.5	102.	2.4
2630–2640	25.1	189	2.5
2640–2650	32.4	243	2.7
2600–2650	95.8×10^3	723	
2650–2660	34.2×10^3	256	2.9×10^{-1}
2660–2670	31.7	236	3.1
2670–2680	33.0	245	3.3
2680–2690	31.8	235	3.4
2690–2700	32.4	238	3.6
2650–2700	163×10^3	1210	

Table 2-2. (*Continued*)

Wavelength Interval Å	$\Phi_{\Delta\lambda}$ (10^9 photons cm^{-2} s^{-1})	$S_{\Delta\lambda}$ mWm^{-2}	$\sum_0^\lambda S_{\Delta\lambda}/S$ %
2700–2710	35.7×10^3	262	3.8×10^{-1}
2710–2710	29.3	214	4.0
2720–2730	26.0	190	4.1
2730–2740	28.6	208	4.2
2740–2750	18.2	132	4.3
2700–2750	138×10^3	1006	
2750–2760	21.2×10^3	153	4.4×10^{-1}
2760–2770	32.1	231	4.6
2770–2780	34.6	248	4.8
2780–2790	24.9	178	4.9
2790–2800	13.3	95	5.0
2750–2800	126×10^3	905	
2800–2810	13.1×10^3	92.8	5.1×10^{-1}
2810–2820	28.9	204	5.2
2820–2830	40.1	282	5.4
2830–2840	44.0	308	5.6
2840–2850	33.9	237	5.8
2800–2850	160×10^3	1124	
2850–2860	22.6×10^3	157	5.9×10^{-1}
2860–2870	46.9	325	6.2
2870–2880	45.7	316	6.4
2880–2890	44.4	306	6.6
2890–2900	63.9	438	7.0
2850–2900	224×10^3	1542	
2900–2910	81.6×10^3	558	7.3×10^{-1}
2910–2910	77.1	525	7.7
2920–2930	68.3	464	8.1
2930–2940	73.9	500	8.4
2940–2950	69.2	467	8.8
2900–2950	370×10^3	2514	
2950–2960	68.1×10^3	458	9.1×10^{-1}
2960–2970	73.6	493	9.5
2970–2980	61.1	408	9.8
1980–2990	64.0	426	1.0×1
2990–3000	64.4	427	1.0
2950–3000	331×10^3	2212	
3000–3010	50.8×10^3	336	1.1
3010–3020	59.3	391	1.1
3020–3030	63.5	417	1.1
3030–3040	77.7	509	1.2
3040–3050	74.9	489	1.2
3000–3050	326×10^3	2142	

Table 2-2. *(Continued)*

Wavelength Interval Å	$\Phi_{\Delta\lambda}$ (10^9 photons cm^{-2} s^{-1})	$S_{\Delta\lambda}$ mWm^{-2}	$\sum_{0}^{\lambda} S_{\Delta\lambda}/S$ %
3050–3060	73.5×10^3	478	1.2
3060–3070	71.9	466	1.3
3070–3080	79.0	510	1.3
3080–3090	76.4	492	1.3
3090–3100	58.5	375	1.4
3050–3100	359×10^3	2321	
3100–3110	78.5×10^3	502	1.4
3110–3120	87.9	561	1.4
3120–3130	78.9	502	1.5
3130–3140	85.3	540	1.5
3140–3150	74.6	471	1.6
3100–3150	405.2×10^3	2576	
3150–3160	66.5×10^3	419	1.6
3160–3170	77.8	488	1.6
3170–3180	105	657	1.7

contributed by the wavelength region shorter than the listed wavelength. For example, the solar irradiance for the entire wavelength region below 3000 Å is 1% of the solar constant.

The solar irradiance based on Table 2-2 is plotted for 20 Å wavelength intervals in Figure 2-3. The pronounced structure for the wavelength Region 1 to 1500 Å arises from emission lines of elements abundant in the sun. The high levels of irradiance in the intervals 300-320 Å and 1200-1220 Å originate primarily from the solar emission lines of He II at 303.78 Å and hydrogen Lyman-α (H Ly-α) at 1215.67 Å, respectively. The solar spectrum above about 1500 Å is essentially a continuum with absorption and emission lines superimposed on the continuum.

2.2.3 Solar Irradiance Below 1200 Å

The temperature of the visible surface of the sun is about 6000 K. If the temperature is measured as a function of distance outward from the surface of the sun, the temperature decreases to about 4500 K at the top of the photosphere (near 500 km) and increases gradually in the chromosphere which extends to about 2000 km. As can be seen in Figure 2-4, the temperature increases rapidly from about 10^4 to 5×10^5 K in a very narrow transition region near 2000 km, and then continues to increase gradually in the corona where the temperature can exceed 2×10^6 K. The solar UV spectrum between 1 and 3000 Å is produced throughout this spatial region which encompasses a temperature range from the photospheric minimum temperature of 4500 K to the coronal temperature of 2×10^6 K.

The solar spectrum between 3000 and 1300 Å is pro-

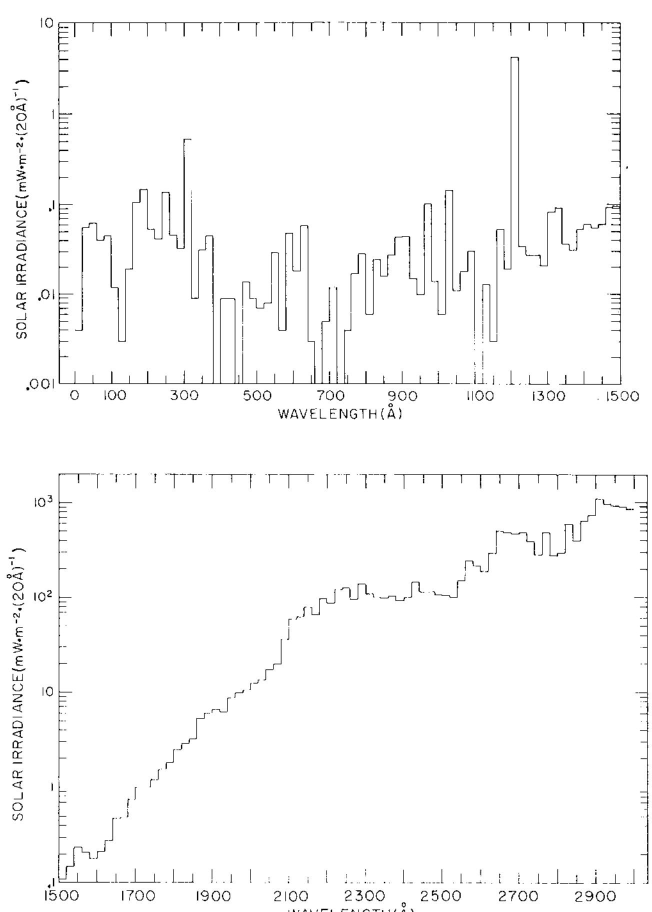

Figure 2-3. The solar spectral irradiance between 1 and 3000 Å for a quiet sun at the top of the earth's atmosphere. The plotted values are averages over 20 Å intervals of wavelength.

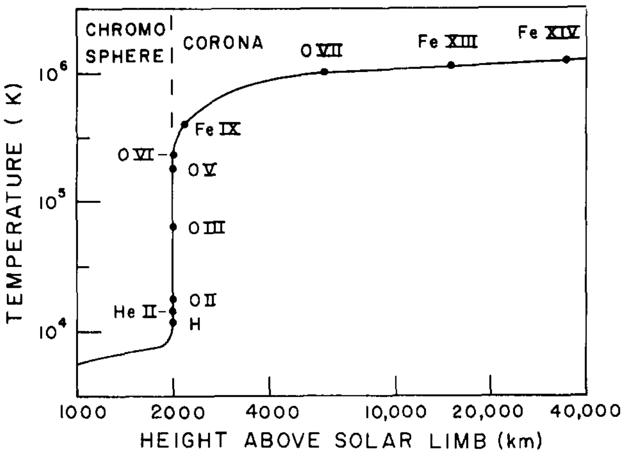

Figure 2-4. The spatial distribution of temperature in the solar chromosphere and corona. The temperature region of production of several multiply-ionized species is also given.

duced predominantly in the upper photosphere and lower chromosphere. The dominant feature in this wavelength region is a continuum that becomes apparent near 1300 Å and increases in intensity toward longer wavelengths as is evident in Figure 2-3. There are numerous emission and absorption lines superimposed on the continuum. At wavelengths shorter than about 1300 Å, the solar spectrum consists predominantly of sharp emission lines that originate from transitions in multiply ionized atomic species that are produced over the wide range of temperatures established in the chromosphere and corona. Figure 2-4 indicates the temperature regions in which several of the ion species observed in the solar spectrum are produced. An example of the solar UV spectrum between 1300 and 270 Å, measured on the NASA OSO 3 satellite by Hall and Hinteregger [1970], is given in Figure 2-5. The scattered light background beneath the spectrum is estimated from a pre-flight calibration to decrease gradually from 150 counts near 120 Å to 50 counts

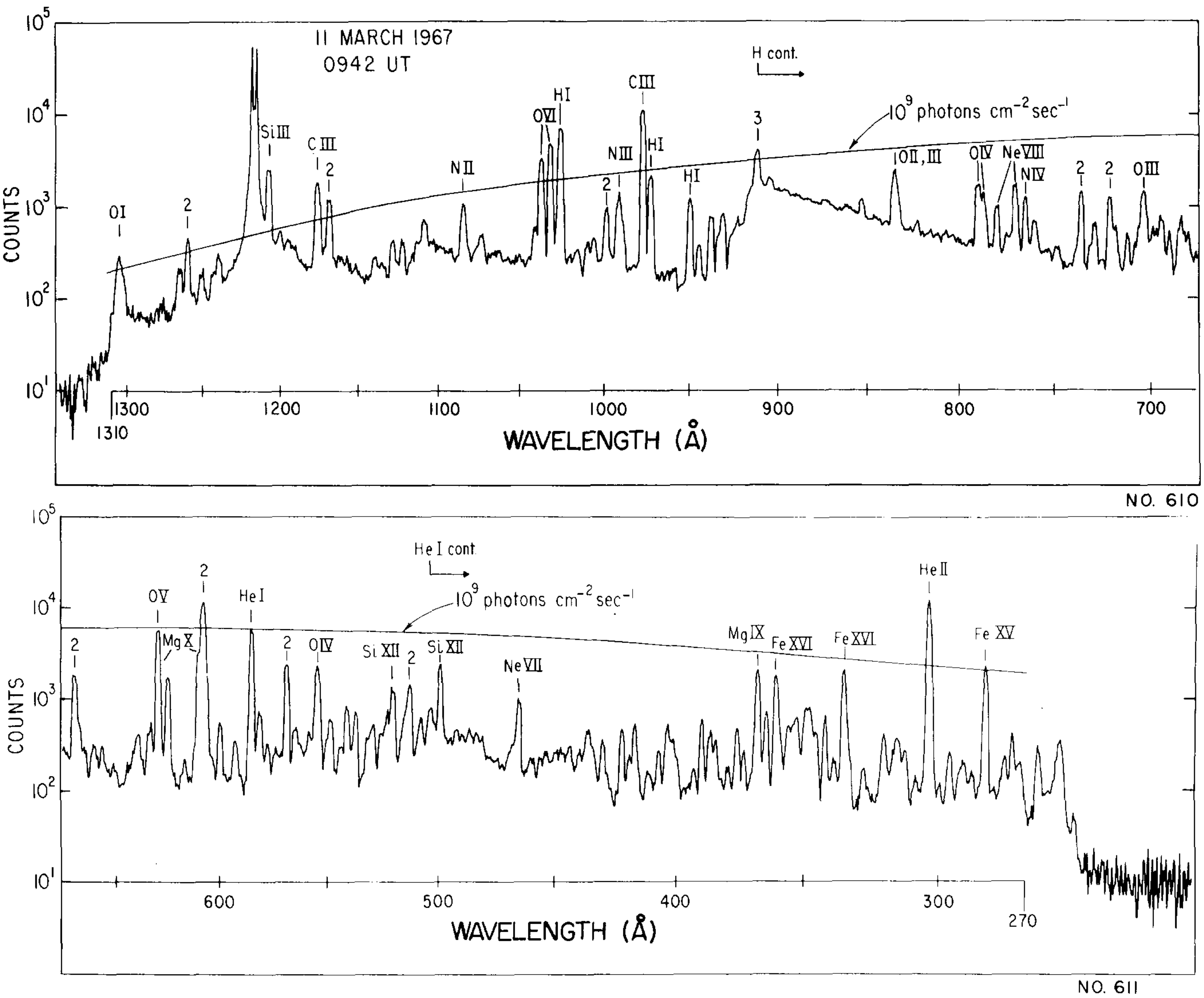

Figure 2-5. The solar UV spectrum between 1300 and 270 Å observed from the satellite OSO 3. The folding of the data for H Ly α line at 1216 Å is introduced by the pulse counting circuitry [Hall and Hinteregger, 1970].

near 270 Å. The reversal of the center of the intense hydrogen Lyman- α line at 1216 Å is instrumental, caused by overflow of the photon counter. The hydrogen continuum which extends from about 911 Å toward shorter wavelengths is the only significant continuum in the spectrum for wavelengths shorter than 1300 Å. A detailed discussion of the spectrum shown in Figure 2-5 is given by Hall and Hinteregger [1970].

The solar UV spectrum between 300 and 100 Å measured in a rocket flight on 4 April 1969 is given in Figure 2-6. The figure is from a paper by Malinovsky and Heroux [1973] where the top of the atmosphere intensities of the lines are also tabulated. For the wavelength interval 300-220 Å, one can see that this small interval of wavelength contains multiplets of ions produced over a wide temperature range extending from 2×10^4 to 2×10^6 K, corresponding to the temperature region of formation of He II and Fe XVI, respectively. The reversal of the intense emission line of Fe XV at 284 Å is again instrumental, caused by overflow of the photon counter.

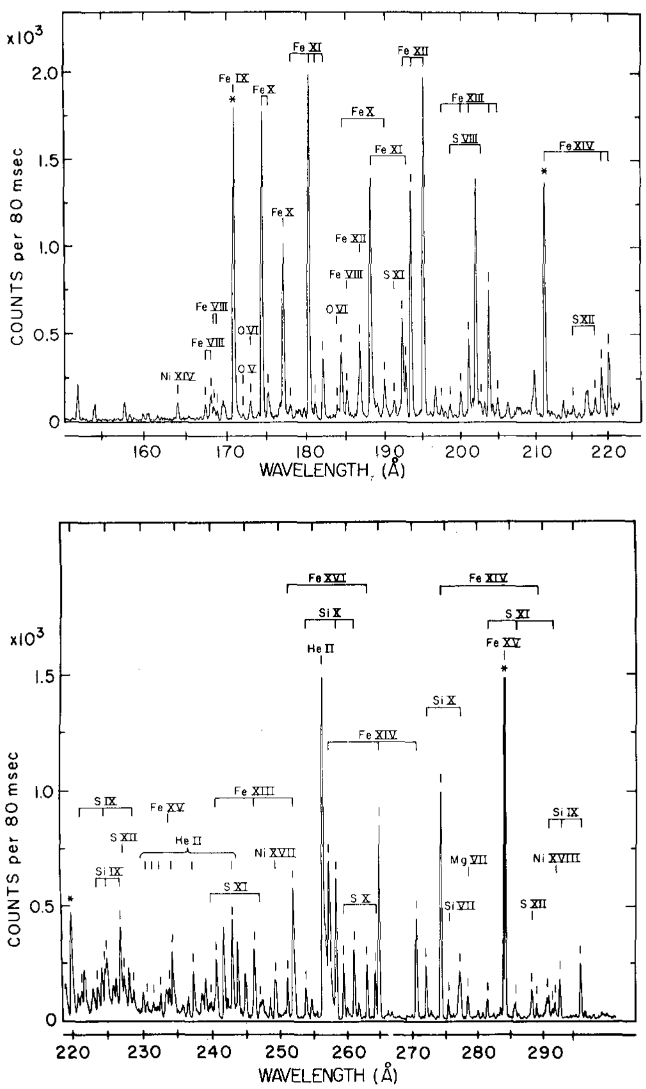

Figure 2-6. The solar UV spectrum between 100 and 300 Å obtained from a rocket flight on 4 April 1969. The folding of the data for the Fe XV line at 284 Å is introduced by the pulse counting circuitry [Malinovsky and Heroux, 1973].

2.3 ABSORPTION OF SOLAR UV

2.3.1 Absorption Below 3200 Å

Solar radiation at wavelengths shorter than about 3200 Å is totally absorbed in the earth's upper atmosphere. Although this ultraviolet region accounts for less than 2% of the total solar irradiance, it is the principal source of energy in the upper atmosphere and controls the neutral and ion composition, temperature, and photochemistry in the stratosphere, mesosphere, and thermosphere. The absorption of solar UV in the earth's atmosphere for an overhead sun is illustrated in Figure 2-7, which gives the altitude at which the rate of absorption at a particular wavelength is a maximum. At these altitudes, solar radiation is reduced by a factor of $e^{-1} = 0.37$ of its value above the earth's atmosphere. The primary atmospheric constituents that absorb the radiation in the different wavelength regions are also given in the figure.

2.3.2 UV Atmospheric/Ionospheric Processes

The absorption of solar UV radiation at wavelengths shorter than 1027 Å ionizes the primary atmospheric constituents O_2, N_2, and O. This radiation is absorbed at altitudes above about 100 km. The rate at which the ions O_2^+, N_2^+ and O^+ are produced as a function of altitude is shown in Figure 2-8. These rates were calculated by using rocket measurements of solar UV intensities for 23 August 1972. The corresponding total production rates of the three species of ions produced by radiation within several wavelength intervals of the solar UV spectrum are given in Figure 2-9. A detailed account of the calculations used to obtain these figures is given by Heroux et al. [1974].

2.4 SOLAR UV IRRADIANCE VARIABILITY

2.4.1 Sunspot Number and 10.7cm Solar Radio Flux

The sunspot number and the 10.7 cm (2800 MHz) solar radio flux are used extensively as indices of solar activity. Eddy [1977] gives a review of sunspot observations that have been made for several hundred years. These records clearly indicate that the sunspots are indicators of solar activity. An additional diagram of the latitudinal distribution of sunspots during the period 1874-1976 is given by Yallop and Hohenkerk [1980]. The sunspot numbers for the present solar cycle 21 are plotted in Figure 2-10. The values are the monthly mean sunspot numbers obtained from the Solar-Geophysical Data Reports published monthly by the Na-

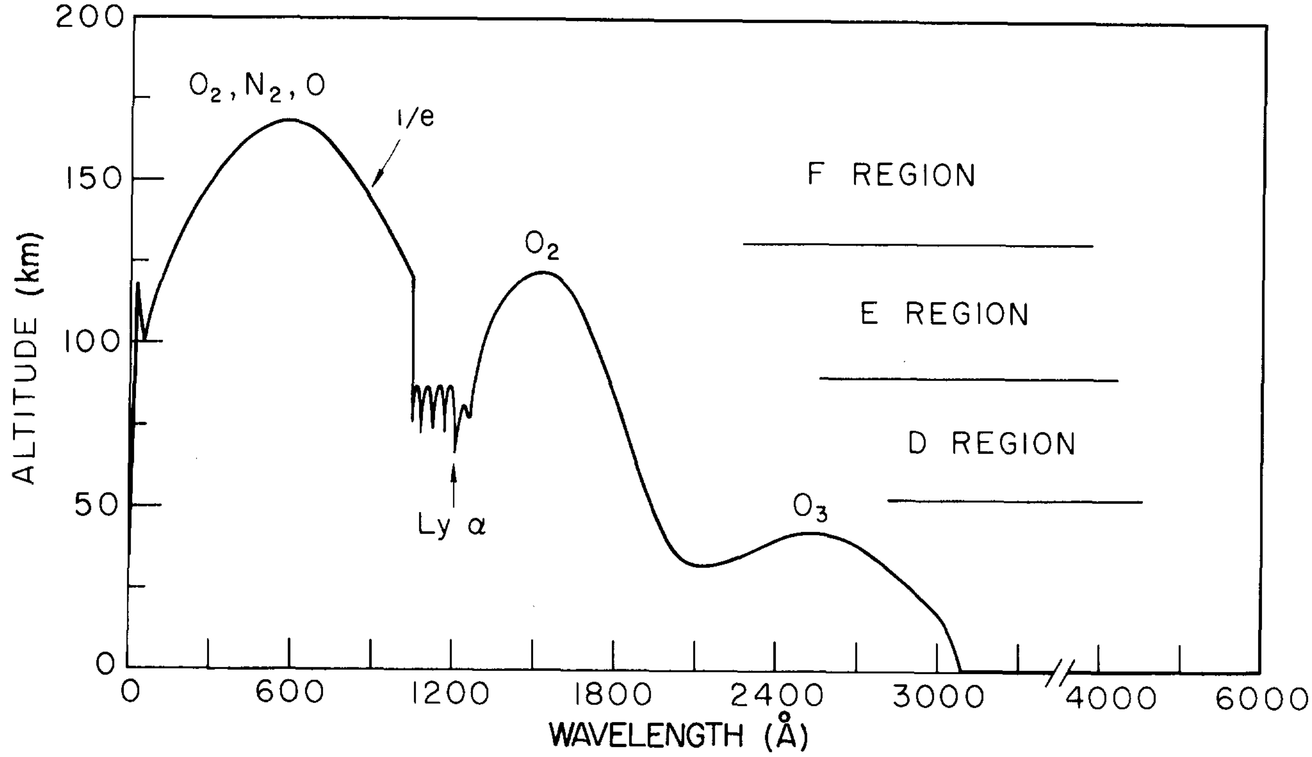

Figure 2-7. The altitude at which the rate of absorption of solar UV radiation is at maximum. The principal atmospheric constituents that absorb the radiation in the different wavelength bands are indicated.

tional Oceanic and Atmospheric Administration (NOAA). These reports also give the daily values of the sunspot numbers. The smoothed mean values of the sunspot numbers for cycles 8-20 are also included in the figure. Each cycle's beginning minimum has been shifted to coincide with the minimum of cycle 21. For comparison, the monthly mean values of the 10.7 cm radio flux for cycle 21 obtained from the NOAA reports are also given in Figure 2-10. Both indices show a similar increase with increasing activity for cycle 21, which began in July 1976. The daily variations

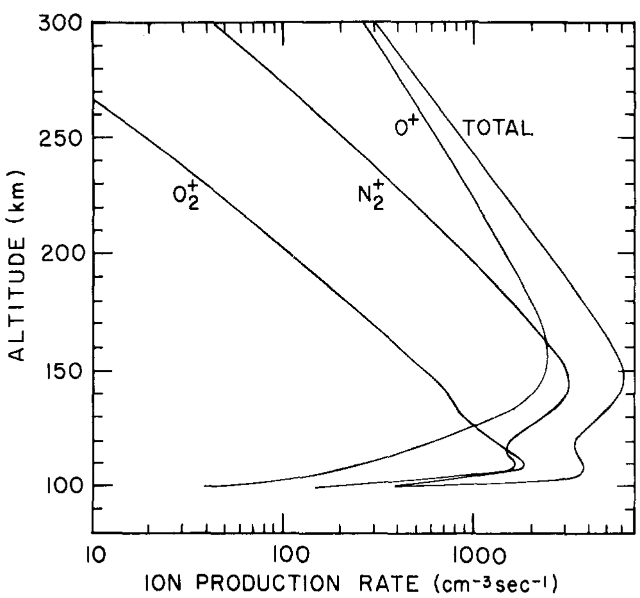

Figure 2-8. Production rates of O^+, $O_2{}^+$, and $N_2{}^+$ and their totals as a function of altitude. The rates were calculated by using rocket measurements of solar intensities between 1027 and 52 Å of 23 August 1972 [Heroux et al., 1974].

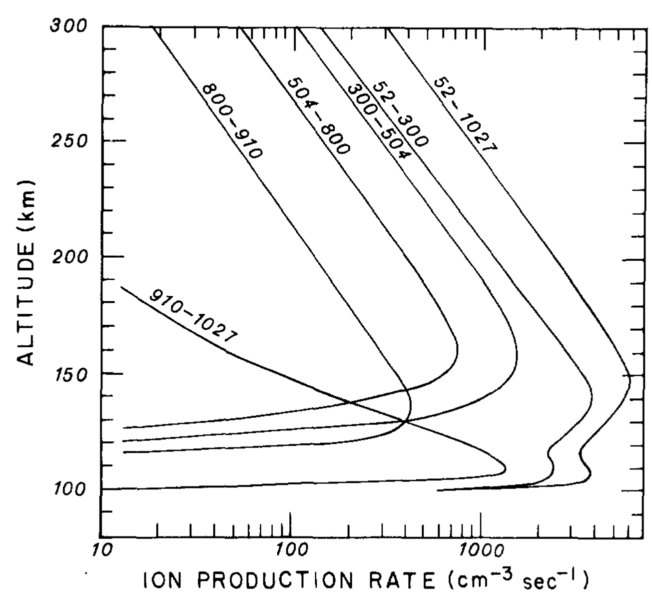

Figure 2-9. Total production rates of O^+, $O_2{}^+$, and $N_2{}^+$ produced by several wavelength regions of the solar UV spectrum. The rates were calculated by using the solar intensities of 23 August 1972 [Heroux et al., 1973].

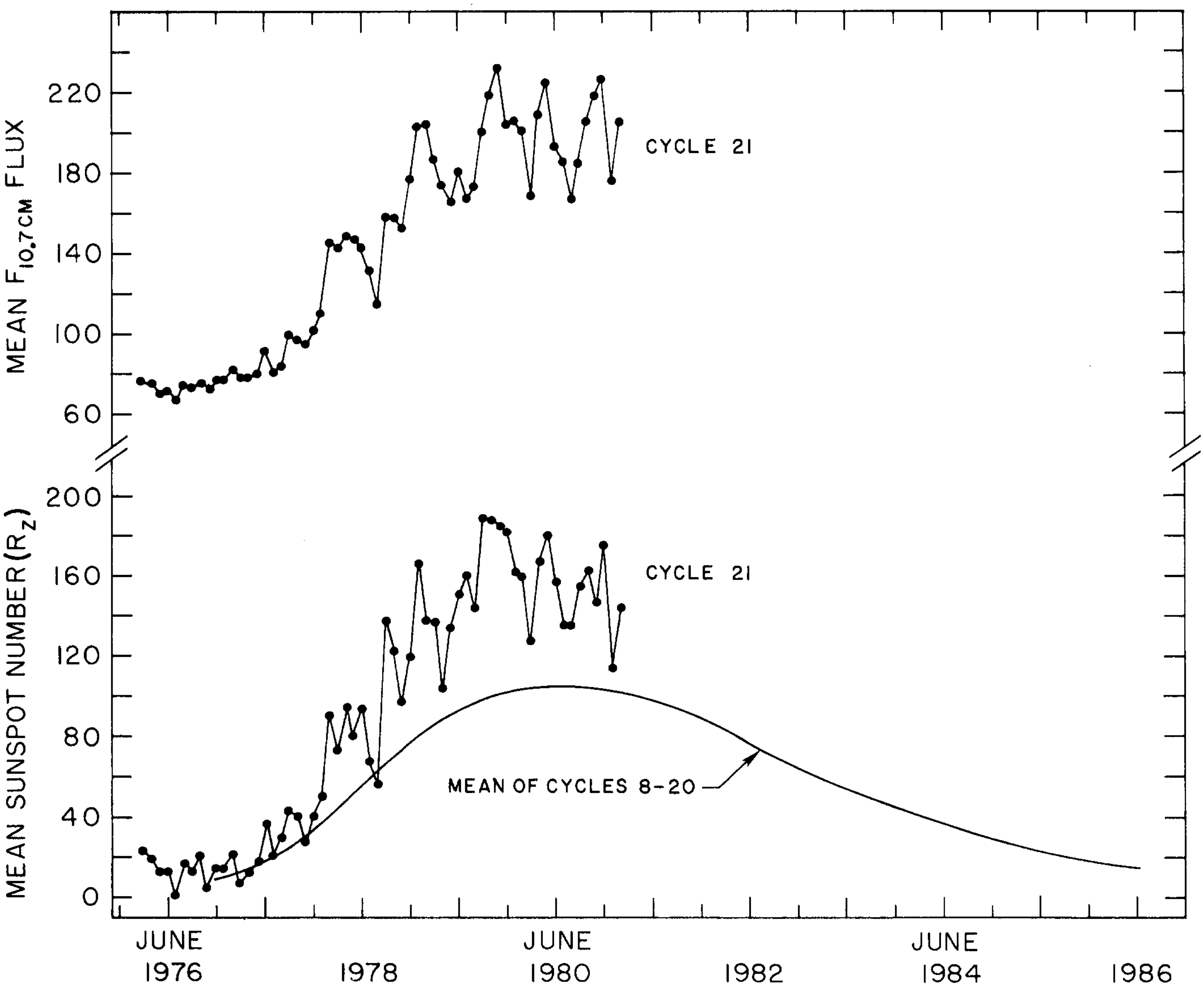

Figure 2-10 Monthly mean sunspot numbers and 10.7 cm radio flux for solar cycle 21, which began in July 1976. The smoothed mean values of the sunspot numbers for cycles 8-20 were obtained by shifting each cycle's minimum value to coincide with the minimum of cycle 21.

in both the sunspot number and the 10.7 cm flux can be significant. For November 1979, the mean value of the sunspot number is 185, while the daily values during the month varied from a minimum value of 98 to a maximum value of 302. For the same month, the mean value of the 10.7 cm flux was 232, while the minimum and maximum values were 154 and 374, respectively.

Although the 10.7 cm flux is a reliable indicator of the general level of solar activity, the correlation between the solar UV flux in narrow wavelength regions and the daily 10.7 cm flux is highly unreliable. Solar UV emissions originate from a wide range of temperatures, densities, and heights in the solar atmosphere extending from the lower chromosphere, the chromosphere-corona transition region, and the corona. The 10.7 cm flux, however, originates predominantly from the upper chromosphere and lower corona. Therefore, it is not surprising that the UV flux emitted from a wide range of regions in the solar atmosphere does not correlate well with the daily 10.7 cm flux emitted from a limited region in the solar atmosphere.

2.4.2 Solar Cycle and UV Variability Below 2000 Å

The variation of the spectral irradiance from the minimum through the maximum level of activity of a solar cycle can be significant for wavelengths shorter than about 1800 Å. This variation is illustrated in Figure 2-11, where the ratio of the irradiance near solar maximum during January 1979 to the irradiance near solar minimum during July 1976 for solar cycle 21 is plotted for 25 Å intervals of wavelength. The data were obtained by Hinteregger [1981] from the

AFGL spectrometer on the NASA Atmosphere Explorer (AE-E) satellite. Figure 2-11 shows that the variation decreases with increasing wavelength toward 1800 Å. At wavelengths longer than about 2300 Å the ratio approaches unity, and therefore solar activity has a negligible effect on the spectral irradiance at these longer wavelengths. The large ratios that are apparent at wavelengths below 500 Å originate from highly ionized atomic species produced in the solar corona. Individual lines that fall within the 25 Å intervals can vary by a significantly higher ratio than that plotted in Figure 2-11 since the plotted ratio represents the irradiance averaged over several lines that fall within the wavelength interval. For example, the ratio of the coronal emission line of Fe XVI at 335.41 Å increases by a factor greater than 100 from solar minimum to maximum, although the ratio of the averaged irradiance in the interval 325-350 Å is a factor of 12.

Figure 2-12 illustrates the relative variation of the solar spectral irradiance for several 50 Å intervals in the 1400-1750 Å range, along with the hydrogen Lyman-α line, at 1216 Å. The variations for the Fe XV 284 Å line emission and for two intervals of the 170-205 Å range are shown in Figure 2-13. These data were obtained on the AE-E satellite by Hinteregger [1980]. Each point represents the average of all measurements for the month. For comparison, the monthly averages of the sunspot number R_z and the 10.7 cm radio emission are included in the figures. These data illustrate that the variation of the irradiance with solar ac-

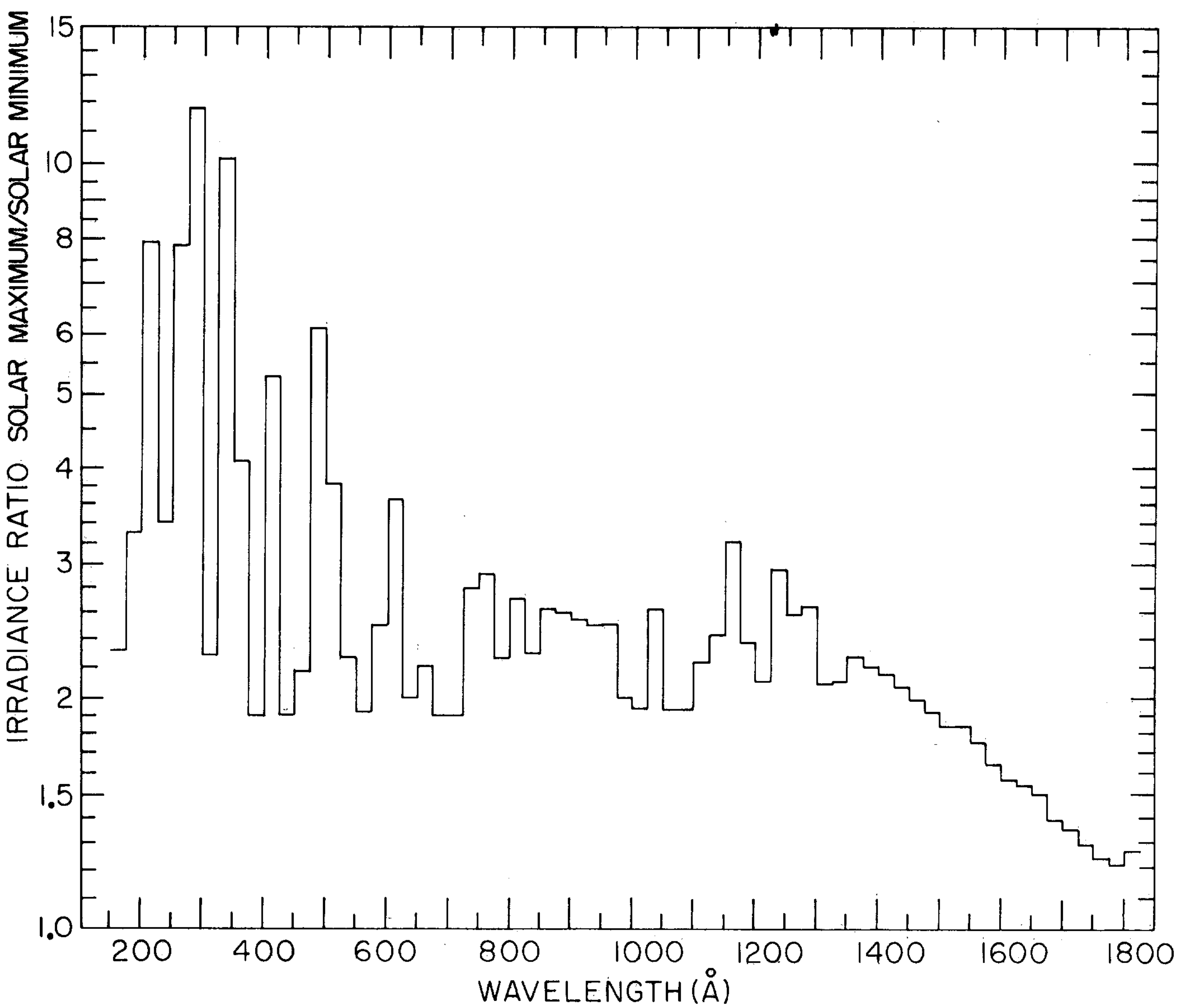

Figure 2-11. The ratio of the solar spectral irradiance near solar maximuim during January 1979 to the irradiance near solar minimum during July 1976 for solar cycle 21. The ratios are plotted for 25 Å intervals of wavelength [Hinteregger, 1981].

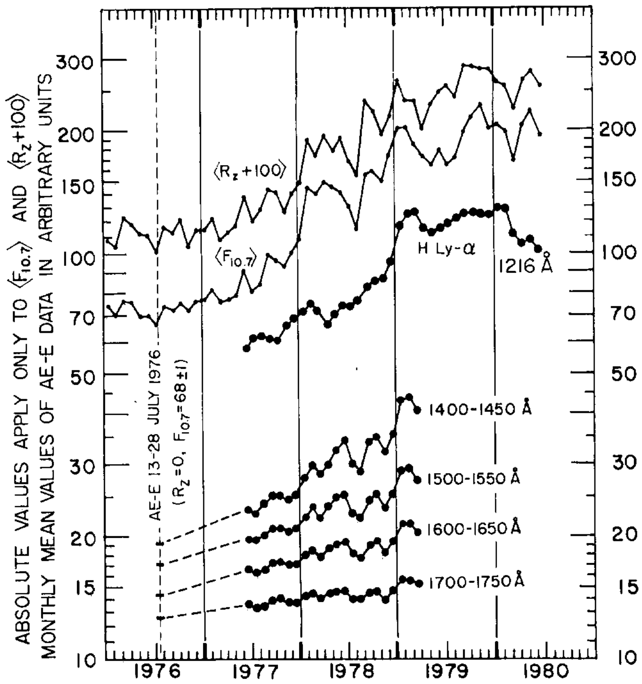

Figure 2-12. Irradiance variations at wavelengths from 1216 to 1750 Å from AE-E satellite measurements during solar cycle 21 [Hinteregger, 1980].

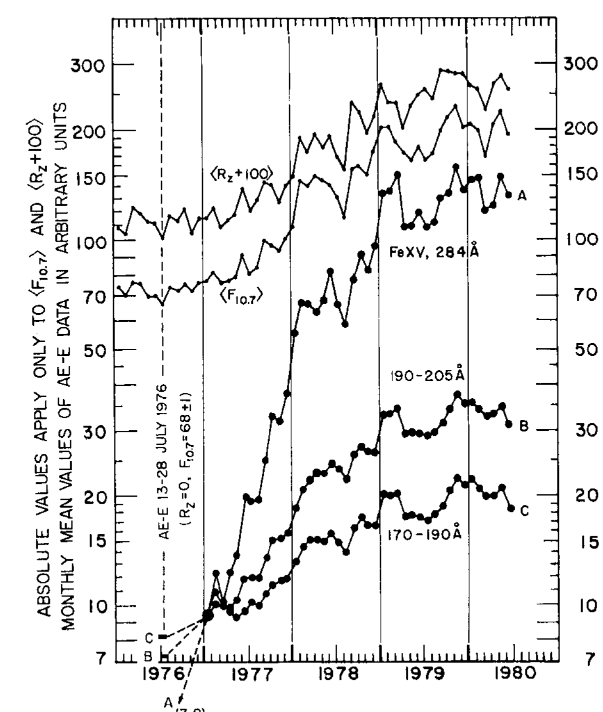

Figure 2-13. Irradiance variations of some solar coronal emissions from AE-E satellite measurements during solar cycle 21 [Hinteregger, 1980].

tivity between 1977 and 1980 depends upon the region of production of the radiation in the solar atmosphere. The variation of the H Lyman-α line that is produced in the lower chromosphere is a factor of approximately 2.3, while the variation of the Fe XV line produced in the corona is approximately 8.0 The variation of the photospheric radiation in the wavelength interval 1700-1750 Å is only 1.16. This variation approaches 1.0 for wavelengths greater than about 2200 Å.

In addition to the variability of the solar UV irradiance over an 11-year cycle, there is also a 27-day variation of solar UV associated with the period of solar rotation. The magnitude of the variation at different wavelengths depends upon the region of the solar atmosphere emitting the radiation. The variations of the emission lines from highly ionized species produced in the corona are significantly greater than the variations of lines produced in the lower chromosphere. This is illustrated in Figure 2-14 where measurements are plotted of the 27-day variation of several solar emission lines for May and June 1967 from an experiment on the OSO 3 satellite [Hall and Hinteregger [1970]. The variation of the coronal Fe XVI lines at 335 Å can be seen to be significantly greater than the variations of the other chromospheric lines shown in the figure. The 27-day variation of the unresolved He II and Si XI lines near 304 Å has also been measured over a period of almost two years (1967 to 1969) from an instrument flown on the OSO 4 satellite by Timothy and Timothy [1970].

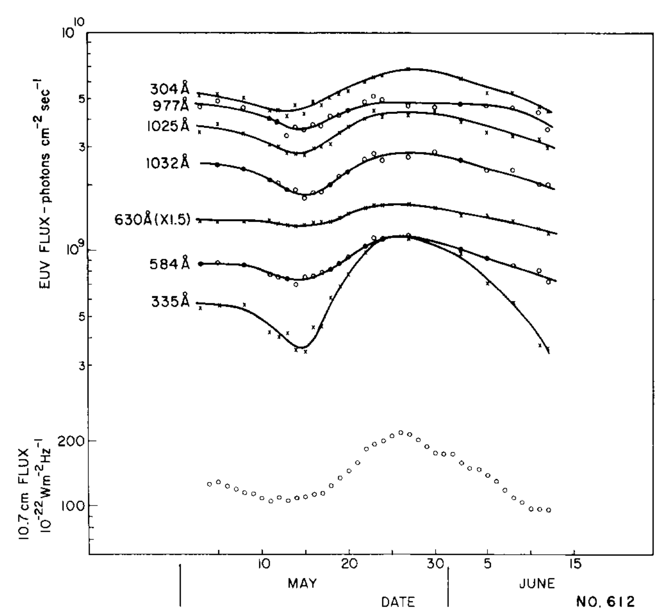

Figure 2-14. The 27-day variations in several UV emission lines observed from the OSO 3 satellite in May and June 1967. The 10.7 cm radio flux for the same period is also given for comparison [Hall and Hinteregger, 1970].

REFERENCES

Delaboudinier, J.P., R.F. Donnelly, H.E. Hinteregger, G. Schmidtke, and P.C. Simon, "Intercomparison/ Compilation of Relevant Solar Flux Data Related to Aeronomy" International Council of Scientific Unions, Committee on Space Research, *COSPAR Technique Manual Series,* **7**:48–51, Paris, 1978.

Eddy, J.A., "Historical Evidence for Existence of the Solar Cycle," in *The Solar Output and Its Variation,* edited by O.R. White, Colorado Associated University Press, Boulder, 1977.

Frohlich, C., "Contemporary Measures of the Solar Constant," in *The Solar Output and its Variation,* edited by O.R. White, Colorado Associated University Press, Boulder, 1977.

Hall, L.A., "Solar Ultraviolet Irradiance at 40 Kilometers in the Stratosphere," *J. Geophys. Res.,* **86:** 555, 1981.

Hall, L.A. and H.E. Hinteregger, "Solar Radiation in the Extreme Ultraviolet and Its Variation with Solar Rotation," *J. Geophys. Res.,* **75:** 6959, 1970.

Heroux, L. and H.E. Hinteregger, "Aeronomical Reference Spectrum for Solar UV Below 2000 Å," *J. Geophys. Res.,* **83:** 5305, 1978.

Heroux, L., M. Cohen, and J.E. Higgins, "Electron Densities Between 110 and 300 km Derived from Solar EUV Fluxes of August 23, 1972," *J. Geophys. Res.,* **79:** 5237, 1974.

Hinteregger, H.E., "Representations of Solar EUV Fluxes for Aeronomical Applications," *Adv. Space Res.,* **1:** 39, COSPAR, 1981.

Hinteregger, H.E., "AE-E Experiences of Irradiance Monitoring for 1250-1850 Å," in *Proceedings of the Workshop on Solar UV Irradiance Monitors,* NOAA Environmental Research Laboratories (ERL), Boulder, 1980.

Kreplin, R.W., K.P. Dere, D.M. Horan, and J.F. Meekins, "The Solar Spectrum Below 10 Å," in *The Solar Output and Its Variation,* edited by O.R. White, Colorado Associated University Press, Boulder, 1977.

Malinovsky, M. and L. Heroux, "An Analysis of the Solar Extreme-Ultraviolet Spectrum Between 50 and 300 Å," *Astrophys. J.,* **181**: 1009, 1973.

Manson, J.E., "The Solar Spectrum Between 10 and 300 Å," in *The Solar Output and Its Variation,* edited by O.R. White, Colorado Associated University Press, Boulder, 1977.

Mount, G.H. and G.J. Rottman, "The Solar Spectral Irradiance 1200-3184 Å Near Solar Maximum: July 15, 1980," *J. Geophys. Res.,* **86:** 9193–9198, 1981.

Pierce, A.K. and R.G. Allen, "The Solar Spectrum Between 0.3 and 10 μm," in *The Solar Output and Its Variation,* edited by O.R. White, Colorado Associated University Press, Boulder, 1977.

Timothy, A.F. and J.G. Timothy, "Long-Term Intensity Variations in the Solar Helium II Lyman Alpha Line," *J. Geophys. Res.,* **75:** 6950, 1970.

Willson, R.C., C.H. Duncan, and J. Geist, "Direct Measurement of Solar Luminosity Variation," *Science,* (London) **207:**177–179, 1980.

Yallop, B.D. and C.Y. Hohenkerk, "Distribution of Sunspots 1874–1976," *Sol. Phys.,* **68:** 303, 1980.